32p

NASA TN D-1549

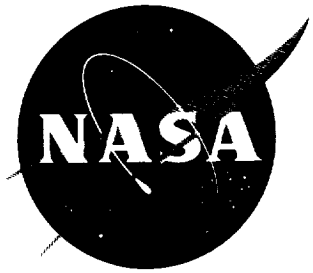

TECHNICAL NOTE

D-1549

ANALYTICAL STUDY OF THE TUMBLING MOTIONS OF VEHICLES ENTERING PLANETARY ATMOSPHERES

By Murray Tobak

Ames Research Center
Moffett Field, Calif.

NATIONAL AERONAUTICS AND SPACE ADMINISTRATION

WASHINGTON

October 1962

NATIONAL AERONAUTICS AND SPACE ADMINISTRATION

TECHNICAL NOTE D-1549

ANALYTICAL STUDY OF THE TUMBLING MOTIONS OF VEHICLES ENTERING PLANETARY ATMOSPHERES

By Murray Tobak

SUMMARY

The tumbling motion of vehicles entering planetary atmospheres is analyzed. A differential equation governing the tumbling motion, its arrest, and the subsequent oscillatory motion is obtained and identified as the equation for the fifth Painlevé transcendant. An approximate analytical solution for the transcendant is derived. Comparisons with results obtained from numerical integration of the exact equations of motion indicate that the solution for the angle-of-attack history is sufficiently accurate to be of practical use.

INTRODUCTION

The oscillatory behavior of vehicles entering planetary atmospheres has been studied intensively in view of its importance in structural and guidance system design. Previous analytical studies, aimed at gaining a clearer understanding of the problem, have been limited to cases where the vehicle either (1) enters the atmosphere without angular velocity (ref. 1) or (2) has progressed far enough into the atmosphere so that any initial tumbling motion has been arrested and the oscillatory motion has been reduced to small excursions from a mean path (refs. 2 to 4). In either case, therefore, the part of the motion history during which the vehicle initially may be tumbling has been excluded from study. This has not been considered a serious limitation, however, since for the vehicles to which the analyses were applied, namely, ballistic missiles and manned spacecraft, it could be assumed that some sort of controlling device would be available to prevent both tumbling and large oscillatory excursions of the angle of attack.

Recently, it has been proposed to send instrumented probe vehicles into the atmospheres of the near-earth planets (ref. 5). It is envisioned that the probe vehicle will be brought to the vicinity of a planet by a larger vehicle and then released. In the interest of simplicity, active control of the probe vehicle's motion after its release would not be provided, the vehicle depending instead on its inherent aerodynamic stability to right itself in the appropriate

orientation after penetrating the planetary atmosphere. It is easy to see that in such a case, the vehicle probably will be tumbling as it enters the atmosphere and that this tumbling motion could play a large role in the design of the vehicle. For example, the weight and extent of the heat shield would depend in great measure on the prediction of the relationship between the altitude range over which the vehicle tumbles and subsequently oscillates with possibly large amplitudes and the altitude range over which heating rates become high. For this problem, the analyses mentioned above are clearly inapplicable. An adequate analytical treatment must provide for the possibility of the vehicle having initially an angular velocity, and for the possibility of its experiencing angle-of-attack oscillations of large amplitude after the tumbling motion is arrested.

A detailed numerical study of the tumbling problem was recently completed for a particular vehicle considered representative of one proposed as a Mars probe (ref. 6). As a corollary to that study, an analytical investigation was undertaken with the intent of defining more clearly the underlying mechanism governing the tumbling motion, its arrest, and the subsequent oscillatory motion. The purpose of this report is to present the results of the analytical investigation.

SYMBOLS

A	reference area
C_D	drag coefficient, $\frac{\text{drag}}{qA}$
C_L	lift coefficient, $\frac{\text{lift}}{qA}$
C_m	pitching-moment coefficient, $\frac{\text{pitching moment}}{qA\ell}$
C_{m_α}	rate of change of pitching-moment coefficient with angle of attack, $\left(\frac{\partial C_m}{\partial \alpha}\right)_{\alpha \to 0}$
$C_{m_{max}}$	maximum value of pitching-moment coefficient
g	acceleration due to gravity
I	pitching moment of inertia about center of gravity
$I_o(x)$	modified Bessel function of first kind of zero order

$J_0(x)$	Bessel function of first kind of zero order
$J_1(x)$	Bessel function of first kind of first order
$Kh_0(x)$	Bessel function of third kind of zero order
$Kh_1(x)$	Bessel function of third kind of first order
$k^2(x)$	parameter defined by equations (19) and (38)
l	body length and reference length for moment-coefficient evaluation
m	vehicle mass
n	integer
q	dynamic pressure, $\frac{1}{2}\rho V^2$
r	distance from center of planet to vehicle
s	dynamic pressure parameter, βv_i
t	time
u	horizontal component of flight velocity (sketch (a))
V	flight velocity (sketch (a))
v	vertical component of flight velocity (sketch (a))
X,Z	axes fixed in space with origin at center of planet (sketch (a))
x	independent variable (eq. (10))
$\bar{x}$	value of x at which $k^2(x) = 1$
$Y_0(x)$	Bessel function of second kind of zero order
$Y_1(x)$	Bessel function of second kind of first order
y	altitude
$Z_0(x)$	$AJ_0(x) + BY_0(x)$
$\tilde{Z}_0(x)$	$\tilde{A}J_0(x) + \tilde{B}Y_0(x)$
$Z_1(x)$	$AJ_1(x) + BY_1(x)$

α	angle of attack (sketch (a))
β	density parameter (eq. (7))
γ	flight-path angle (sketch (a))
ϵ	dependent variable (eq. (16))
η	dependent variable (eq. (35))
Θ	angle of pitch measured from axis fixed in space (sketch (a))
θ	angle of pitch measured from local horizontal (sketch (a))
κ	value of x at $t = 0$ (eq. (10))
ρ	atmospheric density
ρ_o	atmospheric density at surface of planet
τ	value of x at which $x = \kappa e^{-\eta(\kappa)/\kappa\eta'(\kappa)}$
ϕ	angular displacement of vehicle from fixed space axis, $\theta - \Theta$ (sketch (a))
$(\dot{})$	$\frac{d}{dt}( )$
$( )'$	$\frac{d}{dx}( )$
$( )_i$	initial value

ANALYSIS

An analytical study of the tumbling problem is intractable in all generality. Hence, simplifying assumptions must be introduced. It is assumed at the outset that (1) the rotation of the planet and of its atmosphere can be neglected; (2) nothing essential to an understanding of the tumbling motion is lost by considering the motion to be planar; (3) the acceleration due to gravity is constant. Further assumptions and approximations will be introduced as necessary.

Equations of Motion

Under the above assumptions, the equations defining the vehicle's path and its motions about that path may be written as

$$\left.\begin{aligned} -m\dot{V} - C_D qA + mg \sin \gamma &= 0 \\ mV\dot{\gamma} + C_L qA + m\left(\frac{V^2}{r} - g\right)\cos \gamma &= 0 \\ I\ddot{\Theta} - qA\ell C_m &= 0 \end{aligned}\right\} \qquad (1)$$

The angles α, γ, θ, ϕ, Θ are defined in sketch (a).

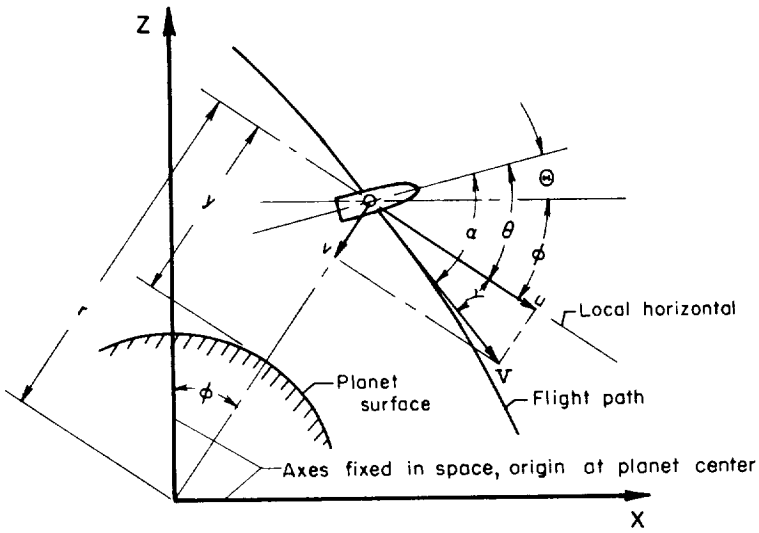

Sketch (a)

Simplified angle-of-attack equation.- Numerical solutions of equations (1) indicate that after the vehicle enters the planetary atmosphere, there is always an interval over which the flight-path angle γ and the flight speed V do not change significantly. Since this is the period of time over which any tumbling motion would occur, it is an appropriate approximation to take

$$\left.\begin{aligned} \gamma &\approx \text{const.} = \gamma_i \\ V &\approx \text{const.} = V_i \end{aligned}\right\} \tag{2}$$

Accordingly, since $\dot{\phi} = u/r$, $\ddot{\phi}$ will be essentially zero, so that

$$\ddot{\theta} \approx \ddot{\alpha} \tag{3}$$

Next, it will be assumed that aerodynamic damping-moment terms are negligible over the range of interest, so that the aerodynamic moment in equations (1) is a function of angle of attack only. This, in conjunction with equation (3), permits the last of equations (1) to be considered independently of the other two. That equation takes the form

$$\ddot{\alpha} - \frac{Al}{I} q(t) C_m(\alpha) = 0 \tag{4}$$

Aerodynamic restoring-moment coefficient.- The fact that the vehicle can be tumbling as it enters the atmosphere requires that the aerodynamic restoring-moment coefficient be specified over the entire angle-of-attack range. It is reasonable to anticipate that heating and stability considerations will dictate the shape of the probe vehicle, hence, that it will be short with a conic profile. Also, in order to minimize the amount of heat protection required, it is advisable that the vehicle be statically stable in one trim position only (cf., ref. 6). Inspection of the experimental results collected in reference 6 for a vehicle satisfying these requirements reveals that the aerodynamic restoring-moment coefficient as a function of angle of attack is approximately a sine wave. Accordingly, it will be assumed that $C_m(\alpha)$ in equation (4) can be approximated by

$$C_m(\alpha) \approx C_{m_{max}} \sin \alpha \tag{5}$$

where $C_{m_{max}}$ is presumed to be available either from experimental data or, for example, from Newtonian impact theory.

Dynamic pressure history.- Consistent with the approximations underlying equations (2), the altitude history of the vehicle as a function of time is

$$y - y_i = -v_i t \tag{6}$$

where

$$v_i = V_i \sin \gamma_i$$

The assumption that the planet's atmospheric density varies exponentially with altitude

$$\rho = \rho_o e^{-\beta y} \tag{7}$$

then gives for the dynamic pressure over the range of interest

$$q(t) = q_i e^{\beta v_i t} \tag{8}$$

with

$$q_i = \frac{1}{2} \rho_o V_i^2 e^{-\beta y_i}$$

Alternatively, if a precise time history of the dynamic pressure is available, a more accurate estimate of q_i and βv_i can be obtained by fitting the best straight line to the initial portion of the dynamic pressure history plotted on semi-logarithmic paper. In this regard, it should be clear that equation (8) reveals one of the apparently more severe limitations of the present analysis; namely, that it can be expected to apply only over the portion of the time history in which $q(t)$ increases uniformly. However, it will be found that this interval encompasses not only the interval over which tumbling occurs, but also the subsequent range over which the oscillatory motion begins and is reduced to small angles. The results of this analysis should be suited to act as the connecting link between the vehicle's initial behavior and the behavior adequately described by the analyses mentioned in the Introduction (refs. 2 to 4).

Transformed equation.- Inserting equations (5) and (8) into equation (4) gives

$$\ddot{\alpha} - q_i \frac{Al}{I} C_{m_{max}} e^{\beta v_i t} \sin \alpha = 0 \tag{9}$$

which will be taken to be the differential equation characterizing the vehicle's motion on entering the atmosphere. However, a transformation of equation (9) yields a form that more quickly shows the nature of the solution. Let

$$\left.\begin{aligned} \beta v_i &= s \\ -q_i \frac{Al}{I} C_{m_{max}} &= \left(\frac{\kappa s}{2}\right)^2 \\ \frac{x}{\kappa} &= e^{st/2} \end{aligned}\right\} \tag{10}$$

Equation (9) takes the form

$$\alpha''(x) + \frac{\alpha'(x)}{x} + \sin \alpha = 0 \tag{11}$$

with the initial conditions

$$\left.\begin{aligned} \alpha(\kappa) &= \alpha_i \\ \alpha'(\kappa) &= \frac{2}{\kappa s}\,\dot{\alpha}_i \end{aligned}\right\} \tag{12}$$

where, for convenience, $\alpha(\kappa)$ is presumed to lie within the range $-\pi \leq \alpha(\kappa) \leq \pi$. Note that all the parameters of the problem have been concentrated in the constant κ and the initial conditions. Equations (11) and (12) indicate that all combinations of vehicle and planetary properties yielding the same value of κ and the same initial conditions $\alpha(\kappa)$, $\alpha'(\kappa)$ will yield identical solutions for α as a function of x, though not necessarily as a function of time.

The Painlevé Transcendants

The substitution $w = \sin \alpha/2$ in equation (11) transforms it to

$$w''(x) = L(w)p^2 + M(x)p + N(w) \tag{13}$$

where

$$p = \frac{dw}{dx}$$

$$L(w) = \frac{w}{w^2 - 1}$$

$$M(x) = -\frac{1}{x}$$

$$N(w) = w(w^2 - 1)$$

In reference 7, it will be found that equation (13) is of the form studied by the French mathematician Paul Painlevé around 1900.[1] It is

[1]It is interesting to note that a Paul Painlevé, professor of mechanics at the École Polytechnique, was the passenger on the Wright brothers' airplane that established a distance record of 34 miles at Le Mans, France, in 1908 (cf., ref. 8).

categorized mathematically as being a member of the general class of second-order differential equations having fixed critical points. This class has been shown to possess 50 members. Of the 50, all but 6 are integrable in terms of known functions. The remaining 6 define new functions, termed "Painlevé transcendants." The substitution $W = (w + 1)/(w - 1)$ casts equation (13) in the form

$$W''(x) = W'^2 \left(\frac{1}{2W} + \frac{1}{W - 1}\right) - \frac{W'}{x} - 2W \left(\frac{W + 1}{W - 1}\right) \qquad (14)$$

and it will be seen in reference 7 that equation (14) is one of these, namely, the fifth. Unfortunately, aside from this categorization, and a comprehensive examination of the asymptotic behavior of the first Painlevé transcendant (ref. 9), no subsequent analyses of their properties seem to have been published. It is hoped that this discovery of an application of at least one of them will stimulate further more purely mathematical study of their properties.

Mechanical Analogy

Before proceeding to develop approximate solutions of equation (9), it may be helpful first to consider a simple mechanical analogy of that equation whose behavior is, in effect, intuitively obvious. By this means, the range and character of motions that a solution of equation (9) will be called upon to describe can be revealed relatively simply.

Consider a small bead constrained to slide, without friction, on a circular path in a vertical plane. Let a time-dependent force $F(t)$ be exerted downward on the bead. This situation is illustrated in sketch (b). Equating the torque about the center of the circle to the bead's rate of change of angular momentum gives

$$\ddot{\varphi} + \frac{1}{r}\left[g + \frac{F(t)}{m}\right] \sin \varphi = 0 \qquad (15)$$

Thus, if $g + F(t)/m$ is caused to vary in proportion to the vehicle's dynamic pressure history, the motion $\varphi(t)$ governed by equation (15) will be analogous to that of the vehicle with φ playing the role of α.

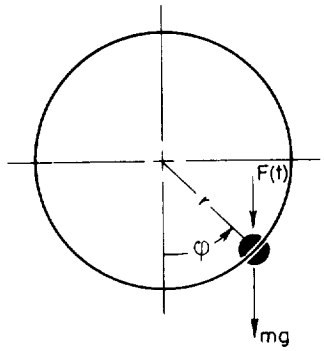

Sketch (b)

For convenience, let $\varphi = 0$ (the bottom of the circle) at $t = 0$. Now give the bead an initial velocity sufficient to carry it several times around the circle. Each time the bead traverses the circle, φ will be counted as having increased by 2π. This, of course, corresponds to one complete tumble of the vehicle. It is clear that, because $F(t)$ continually increases, more and more of the total energy will be in the form of potential energy each time the bead nears the top of the circle. Eventually, therefore, it will not have sufficient kinetic energy to carry it over the top. At this point, it will reverse direction, slide down past the low point, and proceed to oscillate about the low point. Again because the amplitude of the restoring torque grows indefinitely with time, the amplitude of oscillation will diminish and the frequency will increase with time. The final value of φ will be a multiple of 2π. This behavior is illustrated as curve A in sketch (c) for a case where the bead has tumbled twice. Note in the sketch that once tumbling is arrested, the bead's amplitude of oscillation about $2n\pi$ cannot exceed π.[2] For a range of successively smaller initial velocities, the behavior of $\varphi(t)$ will be qualitatively similar to that just described, the tumbling in each case being arrested when φ is between $(2n - 1)\pi$ and $(2n + 1)\pi$ and the subsequent oscillation being about $2n\pi$. Eventually, however, as the initial velocity is successively reduced, a specific initial velocity will be reached for which the kinetic energy near the top of the circle (i.e., $\varphi = (2n - 1)\pi$) is just sufficient to enable the bead to reach the top and come to rest there. The top being a position of unstable equilibrium, the bead cannot oscillate about that position, but must approach it uniformly from below. This is shown as curve B on sketch (c). For a slightly smaller initial velocity, the bead will not surmount the top and, hence, must oscillate about the next smaller multiple of 2π (i.e., $(2n - 2)\pi$). This is shown as curve C on sketch (c). Again, there will be a range of successively smaller initial velocities for which the bead will oscillate about $(2n - 2)\pi$,

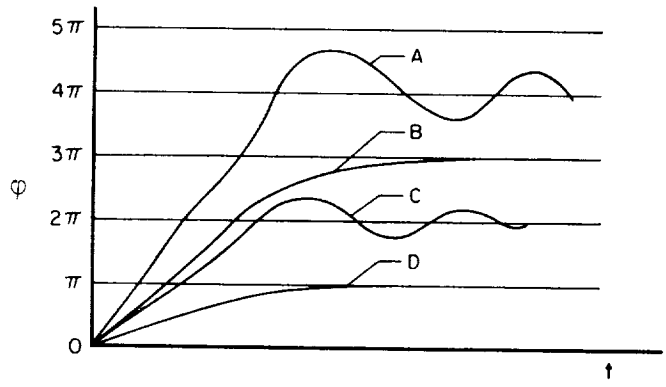

Sketch (c)

[2]It will be observed that this explanation of the arrest of tumbling does not require the presence of aerodynamic damping. This contradicts a result presented in reference 10, in which the cause of the arrest of tumbling is attributed to a dissipation of rotational energy through aerodynamic damping. The author of reference 10 is led to this conclusion by the erroneous assumption that the net change of potential energy over one complete revolution is small enough to be neglected.

eventually terminating with an initial velocity which brings the bead to rest, without oscillating, at $(2n - 3)\pi$ (curve D).

To summarize this discussion as it applies now to the vehicle, it is clear that for any initial angle of attack α_i, there will be a range of values of initial angular velocity $\dot{\alpha}_i$ which will cause α eventually to oscillate about a given value of $2n\pi$. This range of initial angular velocities is bounded by the two specific initial angular velocities which, for the same α_i, cause α to come to rest without oscillating at $(2n + 1)\pi$ and $(2n - 1)\pi$. As discussed in reference 6, these latter cases, where the vehicle comes to rest in a position of unstable equilibrium, are somewhat unrealistic in practice. However, they will be found to be important in analysis, since they serve to define the multiple of 2π about which α eventually oscillates.

Approximate Solutions

The above discussion leads one to anticipate that the solution of equation (11) for cases where α eventually oscillates about an even multiple of π will differ in form from cases where α monotonically approaches an odd multiple of π. Accordingly, the two cases will be treated separately, though by the same procedure.

Oscillatory solution.- Consider equation (11), and to bring in evidence that for the oscillatory solution $\alpha \to 2n\pi$ as $x \to \infty$, let

$$\alpha = 2n\pi - 2\epsilon \tag{16}$$

where, for the time being, n is presumed known. As indicated in the preceding discussion, its value will be determined from the nonoscillatory solution. The equation of motion becomes

$$\epsilon'' + \frac{\epsilon'}{x} + \sin \epsilon \cos \epsilon = 0 \tag{17}$$

where now $\epsilon \to 0$ as $x \to \infty$. A further subdivision of the analysis is now in order to comply with the difference in character between the asymptotic behavior of the solution and the tumbling behavior. The analysis can be divided conveniently on the basis of the following consideration: Multiplying equation (17) by ϵ' and integrating once yields

$$\epsilon'^2(x) = \frac{1}{k^2(x)} \left[1 - k^2(x) \sin^2 \epsilon(x)\right] \tag{18}$$

where

$$k^2(x) = \frac{k_i^2}{1 - 2k_i^2 \int_\kappa^x \frac{\epsilon'^2(u)du}{u}} \tag{19}$$

and

$$k_i^2 = \frac{1}{\epsilon'^2(\kappa) + \sin^2 \epsilon(\kappa)} \tag{20}$$

Let it be assumed first that $k_i^2 < 1$. Equation (19) indicates that $k^2(x)$ must be a continually increasing function. In the interval $k_i^2 \leq k^2(x) \leq 1$, $\sin^2 \epsilon$ varies within the limits $0 \leq \sin^2 \epsilon \leq 1$. But when $k^2(x)$ exceeds unity, equation (18) shows that $\sin^2 \epsilon$ can no longer equal unity, and must diminish as $k^2(x)$ increases. This is the mathematical statement of the condition already noted that once the oscillatory motion has begun, the amplitude of oscillation cannot exceed π. Equation (18) thus reveals that tumbling is arrested and the oscillatory motion begins at the value of x for which $k^2 = 1$. Let this value be $x = \bar{x}$. From equation (18), $\bar{x}$ is determined from the relation

$$\epsilon'(\bar{x}) = \mp \cos \epsilon(\bar{x}) \tag{21}$$

where the negative sign is used with $\epsilon(\kappa) > 0$, the positive sign with $\epsilon(\kappa) < 0$. On the other hand, if $k_i^2 \geq 1$, equations (18) and (19) show that no tumbling occurs; the oscillatory motion begins immediately. Hence, the tumbling motion is confined to the range $\kappa \leq x \leq \bar{x}$, and a solution for this range need be obtained only for values of k_i^2 within the limits $0 < k_i^2 < 1$.

Tumbling behavior: Integrating equation (17) twice yields the integral equation

$$\epsilon(x) = \epsilon(\kappa) + \kappa\epsilon'(\kappa) \log \frac{x}{\kappa} + \int_\kappa^x u \log \frac{u}{x} \sin \epsilon \cos \epsilon \, du \tag{22}$$

Over the range $\kappa \leq x \leq \bar{x}$, an adequate solution of equation (22) can be obtained by successive substitutions. Thus, in the first approximation

$$\epsilon_1(x) = \epsilon(\kappa) + \kappa\epsilon'(\kappa) \log \frac{x}{\kappa} \tag{23}$$

In the second approximation

$$\epsilon_2(x) = \epsilon_1(x) + \int_\kappa^x u \log \frac{u}{x} \sin \epsilon_1(u) \cos \epsilon_1(u)\, du$$

$$= \epsilon_1(x) + L(x) \tag{24}$$

Straightforward integration yields for $L(x)$

$$L(x) = \frac{\kappa^2}{2(4 + c^2)} \left\{ [2 \sin 2\epsilon(\kappa) - c \cos 2\epsilon(\kappa)] \log \frac{x}{\kappa} \right.$$

$$\left. - \left(\frac{x}{\kappa}\right)^2 \sin \left[2\epsilon(\kappa) + c \log \frac{x}{\kappa} - \varphi\right] + \sin [2\epsilon(\kappa) - \varphi] \right\} \tag{25}$$

where

$$c = 2\kappa\epsilon'(\kappa)$$

$$\sin \varphi = \frac{4c}{4 + c^2}$$

$$\cos \varphi = \frac{4 - c^2}{4 + c^2}$$

A third approximation cannot be obtained analytically; fortunately in most cases, the second approximation is sufficiently accurate. An estimate of the magnitude of the third approximation can be obtained since in the interval $\kappa \leq x \leq \bar{x}$, $L(x)$ is generally small. Thus

$$\left.\begin{aligned} \epsilon_3(x) &= \epsilon_1(x) + \frac{1}{2} \int_\kappa^x u \log \frac{u}{x} \sin 2[\epsilon_1(u) + L(u)]\, du \\ &\approx \epsilon_1(x) + \frac{1}{2} \int_\kappa^x u \log \frac{u}{x} [\sin 2\epsilon_1(u) + 2L(u) \cos 2\epsilon_1(u)]\, du \\ &\approx \epsilon_2(x) + \int_\kappa^x u \log \frac{u}{x} L(u) \cos 2\epsilon_1(u)\, du \end{aligned}\right\} \tag{26}$$

The integral can be evaluated in terms of elementary functions. However, as the result is exceedingly lengthy, it will not be presented here. Equation (24) (or (26)) approximates the vehicle's tumbling behavior over the range $\kappa \leq x \leq \bar{x}$, the value of $\bar{x}$ being given by the relation (21).

Oscillatory behavior: The clue which leads to a satisfactory approximation of the oscillatory behavior is again contained in the condition already noted that the amplitude of oscillation cannot

exceed π. Consider the transformation

$$\sin \epsilon = \frac{f(x)}{\sqrt{1 + f^2(x)}} \tag{27}$$

which automatically fulfills this condition. Substitution in equation (17) gives

$$f'' - \frac{2ff'^2}{1 + f^2} + \frac{f'}{x} + f = 0 \tag{28}$$

This is to be compared with the equation for the zero-order Bessel function, in which the nonlinear term is absent. It is anticipated, therefore, that the oscillatory behavior of $f(x)$ should resemble that of the Bessel function. To bring this in evidence, equation (28) is cast in the form of an integral equation by use of the method of variation of parameters. Thus

$$f(x) = Z_o(x) - \frac{\pi}{2}\int_{\bar{x}}^{x} \xi l(\xi) \left[J_o(x)Y_o(\xi) - Y_o(x)J_o(\xi)\right] d\xi \tag{29}$$

where

$$Z_o(x) = AJ_o(x) + BY_o(x)$$

$$l(x) = \frac{2f(x)f'^2(x)}{1 + f^2(x)}$$

The method of successive substitutions, applied to equation (29), then gives to a first approximation

$$f_1(x) = Z_o(x) \tag{30}$$

To a second approximation

$$f_2(x) = Z_o(x) - \frac{\pi}{2}\int_{\bar{x}}^{x} \xi l_1(\xi) \left[J_o(x)Y_o(\xi) - Y_o(x)J_o(\xi)\right] d\xi \tag{31}$$

with

$$l_1(x) = \frac{2Z_o(x)Z_1^2(x)}{1 + Z_o^2(x)}$$

Unfortunately, the integral cannot be evaluated analytically. However, in magnitude it is generally considerably smaller than $Z_o(x)$, and its asymptotic behavior is of no larger order than that of $Z_o(x)$. Therefore, equation (30) alone will be used to represent the oscillatory behavior of $f(x)$.[3] The constants A and B in $Z_o(x)$ are determined by matching equation (30) to the solution for tumbling at $x = \bar{x}$. It will be observed that for large x

$$\sin \epsilon \to \epsilon \to Z_o(x) \tag{32}$$

Comparison of this result with the results of references 1 and 3 reveals that the first approximation to the asymptotic behavior of equation (27) agrees as it should with the previous results obtained under the assumption of small-amplitude oscillations.[4]

Summary of equations: For convenience, the solution for $\epsilon(x)$ over the entire range of x is tabulated below.

$\kappa \leq x \leq \bar{x}$:

$$\epsilon(x) = \epsilon(\kappa) + \kappa\epsilon'(\kappa) \log \frac{x}{\kappa} + L(x)$$

$$L(x) = \frac{\kappa^2}{2(4 + c^2)} \left\{ [2 \sin 2\epsilon(\kappa) - c \cos 2\epsilon(\kappa)] \log \frac{x}{\kappa} \right.$$

$$\left. - \left(\frac{x}{\kappa}\right)^2 \sin \left[2\epsilon(\kappa) + c \log \frac{x}{\kappa} - \varphi \right] + \sin [2\epsilon(\kappa) - \varphi] \right\}$$

$$c = 2\kappa\epsilon'(\kappa)$$

$$\sin \varphi = \frac{4c}{4 + c^2}$$

$$\cos \varphi = \frac{4 - c^2}{4 + c^2}$$

Determine $\bar{x}$ from: $\epsilon'(\bar{x}) = \mp \cos \epsilon(\bar{x})$; $\epsilon(\kappa) \gtrless 0$ (33)

[3]The asymptotic behavior of the integral in both equations (29) and (31) is, in fact, also that of a zero-order Bessel function combination. The true asymptotic behavior of $f(x)$ is therefore, say, $\tilde{Z}_o(x)$, wherein the constants $\tilde{A}$ and $\tilde{B}$ are different from the A and B of equation (30). In the present analysis, however, the added terms are neglected.

[4]The argument of $Z_o(x)$ in equation (30) contains $C_{m_{max}}$ (cf., eq. (10)), whereas in references 1 and 3 the argument of the Bessel functions contains C_{m_α}. For the assumed sinusoidal variation of C_m with α, however, $C_{m_{max}} = (dC_m/d\alpha)|_{\alpha = o}$.

$\bar{x} \leq x$:

$$\left.\begin{aligned} \epsilon(x) &= \sin^{-1}\left[\frac{Z_o(x)}{\sqrt{1 + Z_o^2(x)}}\right] \\ Z_o(x) &= AJ_o(x) + BY_o(x) \\ A &= -\frac{\pi\bar{x}}{2}\left[Y_1(\bar{x}) \tan \epsilon(\bar{x}) + Y_o(\bar{x})\, \epsilon'(\bar{x}) \sec^2 \epsilon(\bar{x})\right] \\ B &= \frac{\pi\bar{x}}{2}\left[J_1(\bar{x}) \tan \epsilon(\bar{x}) + J_o(\bar{x})\, \epsilon'(\bar{x}) \sec^2 \epsilon(\bar{x})\right] \end{aligned}\right\} \tag{34}$$

Finally, it will be recalled that equations (33) and (34) have been derived under the assumption that k_i^2 (eq. (20)) is less than unity. If $k_i^2 \geq 1$, the oscillatory motion begins immediately. In this case, equations (33) can be disregarded and the constants A and B in equations (34) determined directly from the initial conditions; that is, replace $\bar{x}$ by κ in equations (34).

Nonoscillatory solution.- For the nonoscillatory solution, $\alpha \to (2n + 1)\pi$ as $x \to \infty$. To parallel the procedure just described for the oscillatory solution, let

$$\alpha = (2n + 1)\pi - 2\eta \tag{35}$$

The equation of motion becomes

$$\eta'' + \frac{\eta'}{x} - \sin \eta \cos \eta = 0 \tag{36}$$

where $\eta \to 0$ as $x \to \infty$. Note the change in sign from equation (17). Consider first the significance of the parameter k^2. Multiplying by η' and integrating once in equation (36) gives

$$\eta'^2(x) = \frac{1}{k^2(x)}\left[1 - k^2(x) \cos^2 \eta(x)\right] \tag{37}$$

where

$$k^2(x) = \frac{k_i^2}{1 - 2k_i^2 \int_\kappa^x \frac{\eta'^2(\xi)\,d\xi}{\xi}} \tag{38}$$

and

$$k_i^2 = \frac{1}{\eta'^2(\kappa) + \cos^2 \eta(\kappa)} \tag{39}$$

Since it is required that $\eta(x)$ die out to zero for large x, one finds that for the nonoscillatory case, $k^2 \to 1$ as $x \to \infty$. Then k_i^2 must always be less than unity. With $k^2 < 1$ for all x, there is no point $\bar{x}$, as there was in the oscillatory case, at which the solution changes type. Nevertheless, it will be found useful again to divide the solution into two parts - the initial behavior and the asymptotic behavior. Here, however, the point at which the two solutions are joined may be chosen merely on the basis of convenience.

Initial behavior: Integrating equation (36) twice yields

$$\eta(x) = \eta(\kappa) + \kappa\eta'(\kappa) \log \frac{x}{\kappa} - \int_{\kappa}^{x} u \log \frac{u}{x} \sin \eta \cos \eta \, du \tag{40}$$

The approximate solution to equation (40) is obtained again by successive substitutions. To the first approximation

$$\eta_1(x) = \eta(\kappa) + \kappa\eta'(\kappa) \log \frac{x}{\kappa} \tag{41}$$

To the second approximation

$$\eta_2(x) = \eta_1(x) - M(x) \tag{42}$$

where

$$M(x) = \int_{\kappa}^{x} u \log \frac{u}{x} \sin \eta_1(u) \cos \eta_1(u) \, du \tag{43}$$

Note that the solution given for $L(x)$ (eq. (25)) applies also to $M(x)$ where now $c = 2\kappa\eta'(\kappa)$ and $\epsilon(\kappa)$ is replaced by $\eta(\kappa)$. A convenient stopping point for the initial behavior is the value of x at which the first approximation, equation (41), passes through zero. For then, with $\eta(\kappa) > 0$, the second approximation yields a small positive value at this point, which provides the necessary starting value for the nonoscillatory asymptotic behavior; that is, η approaching zero from above as $x \to \infty$. Let the value of x be $x = \tau$. Then

$$\tau = \kappa e^{-\eta(\kappa)/\kappa\eta'(\kappa)} \tag{44}$$

Asymptotic behavior: The substitution

$$\sin \eta = \frac{g(x)}{\sqrt{1 + g^2(x)}} \tag{45}$$

in equation (36) yields

$$g'' - \frac{2gg'^2}{1 + g^2} + \frac{g'}{x} - g = 0 \tag{46}$$

which is to be compared with the differential equation for the zero-order Bessel function of imaginary argument. Casting equation (46) in the form of an integral equation gives

$$g(x) = CI_0(x) + DKh_0(x) - \frac{\pi}{2}\int_x^\infty \xi m(\xi)\,[I_0(x)Kh_0(\xi) - Kh_0(x)I_0(\xi)]d\xi \tag{47}$$

where

$$m(x) = \frac{2g(x)g'^2(x)}{1 + g^2(x)}$$

and the notation for the Bessel functions follows that of Jeffreys (ref. 11). Then to a first approximation

$$g(x) \approx CI_0(x) + DKh_0(x) \tag{48}$$

It is recalled, however, that $\eta(x)$ must approach zero as $x \to \infty$, whereas $I_0(x) \to \infty$ as $x \to \infty$. Therefore, C must equal zero. Then there is only one arbitrary constant, D, and this is as it should be, since for any $\alpha(\kappa)$ there is only one $\alpha'(\kappa)$ that will bring the motion to rest at a given odd multiple of π. That is, when $\eta(\kappa)$ is specified, $\eta'(\kappa)$ is determined, or vice versa. Finally, the constant D is to be determined by matching equation (48) to the solution for the initial behavior, equation (42), at $x = \tau$. This calculation will provide the means of determining the relationship between $\eta(\kappa)$ and $\eta'(\kappa)$, which in turn determines the appropriate value of n to be used in the initial condition $\epsilon(\kappa)$ of the oscillatory solution.

Relationship between $\eta(\kappa)$ and $\eta'(\kappa)$: Matching equations (42) and (45) in magnitude and slope at $x = \tau$ yields two expressions

$$\left.\begin{aligned} \sin\,\eta(\tau) &= \frac{DKh_0(\tau)}{[1 + D^2Kh_0^2(\tau)]^{1/2}} \\ \eta'(\tau) &= \frac{-DKh_1(\tau)}{1 + D^2Kh_0^2(\tau)} \end{aligned}\right\} \tag{49}$$

where, from equation (42)

$$\left.\begin{aligned} \eta(\tau) &= -M(\tau) \\ \eta'(\tau) &= \frac{\kappa\eta'(\kappa)}{\tau} - M'(\tau) \end{aligned}\right\} \tag{50}$$

Eliminating D yields

$$\frac{\sin 2\eta(\tau)}{2\eta'(\tau)} = -\frac{Kh_0(\tau)}{Kh_1(\tau)} = \frac{-\sin 2M(\tau)}{\frac{2}{\tau}\kappa\eta'(\kappa) - 2M'(\tau)} \tag{51}$$

Since $\tau = \kappa e^{-\eta(\kappa)/\kappa\eta'(\kappa)}$, it is the solution of equation (51) which gives the desired relationship between $\eta(\kappa)$ and $\eta'(\kappa)$. Without additional approximation, equation (51) must be solved by trial and error. Further simplification, however, will reveal the nature of the relationship. Since $\eta(\tau)$ is small

$$\frac{\sin 2\eta(\tau)}{2\eta'(\tau)} \approx \frac{\eta(\tau)}{\eta'(\tau)} \approx -\frac{\tau M(\tau)}{\kappa\eta'(\kappa) - \tau M'(\tau)} \tag{52}$$

Also, for any value of τ not close to zero

$$\frac{Kh_0(\tau)}{Kh_1(\tau)} \approx 1 \tag{53}$$

Equation (52) becomes

$$M(\tau) + M'(\tau) \approx \frac{\kappa\eta'(\kappa)}{\tau} \tag{54}$$

which may be written, using equations (41) and (43)

$$\int_\kappa^\tau u\left(\log\frac{u}{\tau} - \frac{1}{\tau}\right)\sin 2(a + b\log u)\,du \approx \frac{2b}{\tau} \tag{55}$$

with

$$a = \eta(\kappa) - \kappa\eta'(\kappa)\log\kappa = -\kappa\eta'(\kappa)\log\tau$$

$$b = \kappa\eta'(\kappa)$$

The change in variables $u = \omega\tau$ gives

$$\int_{\kappa/\tau}^{1} \omega \left(\log \omega - \frac{1}{\tau}\right) \sin (2b \log \omega)\, d\omega \approx \frac{2b}{\tau^3} \tag{56}$$

Since κ/τ is small (the order of 0.1 for the cases studied in ref. 6) and the integrand is near zero for small ω, extending the lower limit of the integral to zero causes only a small error. Let $y = 4(1 + b^2)$. The integration then leads to a quadratic equation in y

$$y^2 - \tau^2 y - 4\tau^3 = 0 \tag{57}$$

The approximate relation between $\eta(\kappa)$ and $\eta'(\kappa)$ is of the form

$$\kappa\eta'(\kappa) \approx \mp \sqrt{\frac{\tau^2}{8}\left(1 + \sqrt{1 + \frac{16}{\tau}}\right) - 1} \tag{58}$$

where, for the radical to be real, $\tau \geq 1.315$. It is of interest to note the implication of equation (58) that $\kappa\eta'(\kappa)$, when written as a function of the parameter τ, may be independent of κ, at least for small values of κ. To investigate this possibility, as well as the accuracy of equation (58), the relationship between $\eta(\kappa)$ and $\eta'(\kappa)$ was also obtained for several values of κ by a trial and error procedure of numerically integrating the Painlevé equation (36).[5] The results, plotted as a function of τ, are shown on figure 1 together with the approximate solution, equation (58). A close inspection of the curves reveals that the numerical results contain oscillatory components which grow as κ increases. Over the range $0 < \kappa < 0.3$, however, the curves are essentially identical. It is surprising to note also that despite the many approximations involved in the derivation of equation (58), the solution adequately describes the form of the numerical results. Of course, in use, the numerical results are to be preferred over equation (58). The result is used as follows: Observing that $2\eta'(\kappa) = -\alpha'(\kappa)$, one uses figure 1 to prepare a curve of $2\eta(\kappa)$ versus $\alpha'(\kappa)$ such as shown in sketch (d). Suppose, for example, it is given that $\alpha(\kappa) = \pi/2$, $\alpha'(\kappa) = \zeta_1$. Since $2\eta(\kappa)$ is equal to $\alpha(\infty) - \alpha(\kappa)$, where $\alpha(\infty)$ must be an odd multiple of π (eq. (35)), one finds from the curve that the vehicle will come to rest at $\alpha(\infty) = \pi$ (i.e., $2\eta(\kappa) = \pi/2$) for an initial angular velocity of $\alpha_1'(\kappa)$, whereas for an initial angular velocity of $\alpha_2'(\kappa)$ the vehicle comes to rest at $\alpha(\infty) = 3\pi$ (i.e., $2\eta(\kappa) = 5\pi/2$). Then it is indicated that for $\alpha(\kappa) = \pi/2$, any initial angular velocity between $\alpha_1'(\kappa)$ and $\alpha_2'(\kappa)$ will cause the vehicle to oscillate about $\alpha = 2\pi$. The given value ζ_1 lies between these limits; hence, the

[5]The general solution of equation (36) contains two arbitrary constants whereas for the solutions required here the constants are interdependent. The numerical integration therefore entailed a trial and error procedure wherein for each $\eta(\kappa)$ chosen the value of $\eta'(\kappa)$ was varied until the specific $\eta'(\kappa)$ was found which caused the solution $\eta(x)$ to approach zero asymptotically within a specified error.

appropriate value of n to be used in the oscillatory solution is $n = 1$. As a second example, suppose again that $\alpha(\kappa) = \pi/2$, but that $\alpha'(\kappa)$ is a smaller value, ζ_2, such that in equation (20), $k_i^2 > 1$. As indicated on the sketch, the initial angular velocity $\alpha_1'(\kappa)$ brings the vehicle to rest at $\alpha(\infty) = \pi$, whereas the initial angular velocity $\alpha_3'(\kappa)$ brings the vehicle to rest at $\alpha(\infty) = -\pi$. Since ζ_2 lies between $\alpha_1'(\kappa)$ and $\alpha_3'(\kappa)$, it is indicated that $\alpha(\infty) = 0$; hence, $n = 0$. Since $k_i^2 > 1$, one uses equation (34) alone for the oscillatory solution as previously noted.

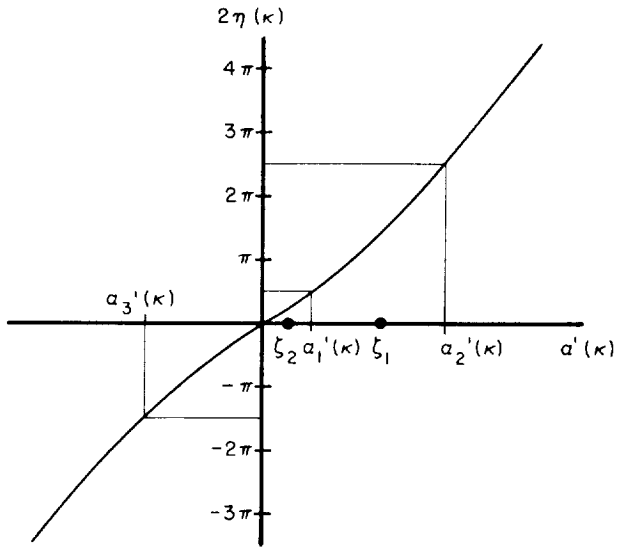

Sketch (d)

Finally, to complete the nonoscillatory solution, having determined τ from figure 1, one finds the constant D for use in equation (48) from

$$D = \frac{1}{Kh_0(\tau)} \tan \eta(\tau) \tag{59}$$

Summary of equations:

$\kappa \leq x \leq \tau$:

$$\left.\begin{aligned}
&\eta(x) = \eta(\kappa) + \kappa\eta'(\kappa) \log \frac{x}{\kappa} - M(x) \\
&M(x) = \frac{\kappa^2}{2(4 + c^2)} \left\{ [2 \sin 2\eta(\kappa) - c \cos 2\eta(\kappa)] \log \frac{x}{\kappa} \right. \\
&\qquad \left. - \left(\frac{x}{\kappa}\right)^2 \sin \left[2\eta(\kappa) + c \log \frac{x}{\kappa} - \varphi\right] + \sin [2\eta(\kappa) - \varphi] \right\} \\
&c = 2\kappa\eta'(\kappa) \\
&\sin \varphi = \frac{4c}{4 + c^2} \\
&\cos \varphi = \frac{4 - c^2}{4 + c^2} \\
&\tau = \kappa e^{-\eta(\kappa)/\kappa\eta'(\kappa)}
\end{aligned}\right\} \tag{60}$$

$\tau \leq x$:

$$\left.\begin{aligned} \eta(x) &= \sin^{-1}\left[\frac{DKh_o(x)}{\sqrt{1 + D^2Kh_o^2(x)}}\right] \\ D &= \frac{1}{Kh_o(\tau)} \tan \eta(\tau) \end{aligned}\right\} \tag{61}$$

Approximate $\eta'(\kappa)$:

$$\kappa\eta'(\kappa) \approx \mp\sqrt{\frac{\tau^2}{8}\left(1 + \sqrt{1 + \frac{16}{\tau}}\right) - 1}\,; \qquad \tau \geq 1.315 \tag{62}$$

Numerical Comparisons

In assessing the adequacy of the analysis presented here, it is necessary to note that two sorts of approximations are involved: First, the Painlevé equation is itself an approximation to the complete equations of motion, and, second, it was necessary to introduce additional approximations to obtain analytic solutions of the Painlevé equation. To determine whether the final results are still of sufficient accuracy to be useful, numerical results will be compared with a few of the results of reference 6, in which no approximations were made, either to the equations of motion or to the aerodynamic forces and moments. This comparison will also afford a means of demonstrating the use of the analytical results.

Calculation of parameters.- The vehicle studied in reference 6 had the following physical properties

$$\left.\begin{aligned} A &= 8.296 \text{ ft}^2 \\ I &= 5.6 \text{ lb-ft-sec}^2 \\ l &= 3.25 \text{ ft} \\ C_{m_{max}} &= -0.1876 \end{aligned}\right\} \tag{63}$$

Flight conditions on entering the Martian atmosphere were

$$\left.\begin{aligned} y_i &= 800{,}000 \text{ ft} \\ V_i &= 21{,}042 \text{ ft/sec} \\ \gamma_i &= 41.5^\circ \end{aligned}\right\} \tag{64}$$

A semilogarithmic plot of the dynamic pressure history, taken from reference 6, is given on figure 2. It is clear from the figure that equation (8) is an excellent approximation of the dynamic pressure history almost until the time at which q becomes maximum. It is indicated that the analytical results should be applicable over at least the first 45 seconds of flight after entry. The values of q_i and βv_i are obtained from the initial value and slope of figure 2. The parameter κ is then calculated from equation (10).

$$\left.\begin{aligned} q_i &= 1.23\times10^{-3} \text{ lb/ft}^2 \\ \beta v_i &= s = 0.30 \text{ per sec} \\ \kappa &= 0.222 \end{aligned}\right\} \tag{65}$$

Case 1.- Consider first a case representative of the results presented in reference 6. Let

$$\left.\begin{aligned} \alpha_i &= -\pi \\ \dot{\alpha}_i &= 12^\circ/\text{sec} = 0.2094 \text{ radian/sec} \\ \alpha'(\kappa) &= \frac{2}{\kappa s}\dot{\alpha}_i = 6.29 \end{aligned}\right\} \tag{66}$$

The first step in obtaining the analytical solution is to determine the value of α about which the vehicle ultimately oscillates. Figure 1 is used to prepare a curve of $2\eta(\kappa)$ vs. $\alpha'(\kappa)$. The result for $\kappa = 0.222$ is given on figure 3 (only one branch of the curve is shown since $\eta(\kappa)$ is antisymmetric with respect to $\alpha'(\kappa)$). With $\alpha(\kappa) = -\pi$, it is found from figure 3 that the vehicle will come to rest at $\alpha(\infty) = \pi$ (i.e., $2\eta(\kappa) = 2\pi$) for $\alpha'(\kappa) = 12.1$, whereas the vehicle will remain at rest at $\alpha(\infty) = -\pi$ (i.e., $2\eta(\kappa) = 0$) for $\alpha'(\kappa) = 0$. Since the given initial rate $\alpha'(\kappa) = 6.29$ lies between these limits, it is indicated that the vehicle will oscillate about $\alpha = 0$. Then $n = 0$ in equation (16). One then uses equations (33) and (34) to compute the motion. The results are shown on figure 4, compared with the result of reference 6 and the result of numerically integrating the Painlevé equation, equation (17). It will be observed first that the numerical solution of the Painlevé equation is capable of accurately depicting the exact result. Also, while the approximate analytical solution of the Painlevé equation introduces an additional error, it does not appear to be of serious magnitude. A useful measure of the agreement between the three results is the magnitude and time of occurrence of the first peak of oscillation; the numerical solution of the Painlevé equation gives 55° at 17.5 sec, the approximate solution gives 60° at 17.1 sec, whereas the exact result is 57° at 17.8 sec.

Case 2.- As a second example, consider an extreme case where the vehicle is given an initial angular velocity several times larger than those within the range of values considered likely in reference 6. Let

$$\left.\begin{aligned} \alpha_i &= 0 \\ \dot{\alpha}_i &= 86^\circ/\text{sec} = 1.5 \text{ radians/sec} \\ \alpha'(\kappa) &= 45.05 \end{aligned}\right\} \tag{67}$$

For the analytic solution, reference to figure 3 reveals that the vehicle would come to rest at $2\eta(\kappa) = \alpha(\infty) = 13\pi$ for $\alpha'(\kappa) = 50.6$, and at $2\eta(\kappa) = \alpha(\infty) = 11\pi$ for $\alpha'(\kappa) = 44.4$. Since the given initial rate $\alpha'(\kappa) = 45.05$ lies between these boundaries, it is indicated that the vehicle ultimately oscillates about $\alpha = 12\pi$; that is, $n = 6$ in equation (16). The motion is computed from equations (33) and (34). The results are shown on figure 5. Only the last part of the tumbling motion is shown, since over the initial portion of the time interval during which the vehicle tumbles, all three results indicate the same thing, namely that $\alpha(t) \approx \alpha_i + \dot{\alpha}_i t$. It is evident from inspection of figure 5 that even for this extreme case, the numerical solution of the Painlevé equation is in adequate agreement with the exact result. The approximate analytical solution for tumbling (eq. (24)) properly indicates the large change in curvature that occurs just before the vehicle passes through 11π, but fails to predict its full extent. As a result, the analytical prediction of the first peak of oscillation is in error by some 27°. The marked slowdown of the motion at the odd multiple of π is caused by the fact that $\alpha'(\kappa)$ is very near its lower boundary (cf., fig. 3); that is, the vehicle tends to dwell near its position of unstable equilibrium at 11π. Using the next approximation for the tumbling motion, equation (26), brings the analytical solution more closely in line with this behavior. Nevertheless, this result should be taken as warning that both the numerical solution of the Painlevé equation and the analytical prediction will become progressively less trustworthy as $\alpha'(\kappa)$ approaches nearer and nearer one of its boundary values. In fact, since the agreement between a curve such as figure 3 and the exact curve will not be perfect, eventually it can happen that while one curve indicates the vehicle will oscillate about some multiple of 2π, the other curve may indicate the vehicle will oscillate about one higher or one lower multiple of 2π. On the other hand, the condition where the vehicle tends to or actually reaches a position of unstable equilibrium generally can be disregarded on practical grounds, for the reasons discussed in reference 6. For the remaining cases, solutions of the Painlevé equation should give results of the order of accuracy illustrated in figure 4.

CONCLUDING REMARKS

An analytical study has been made of the tumbling motions of vehicles entering planetary atmospheres. A simplified differential equation governing the tumbling motion, its arrest, and the subsequent oscillatory motion was obtained and identified as the equation for the fifth Painlevé transcendant. An approximate analytical solution for the transcendant was derived. Results from this solution were compared with numerical solutions of the Painlevé equation and with solutions obtained from numerical integration of the exact equations of motion. The results for angle-of-attack history indicated that both the numerical solution of the Painlevé equation and its approximate analytical solution were of sufficient accuracy to be of use in practical computations.

Ames Research Center
National Aeronautics and Space Administration
Moffett Field, Calif., July 17, 1962

REFERENCES

1. Allen, H. Julian: Motion of a Ballistic Missile Angularly Misaligned With the Flight Path Upon Entering the Atmosphere and Its Effect Upon Aerodynamic Heating, Aerodynamic Loads, and Miss Distance. NACA TN 4048, 1957.

2. Friedrich, Hans R., and Dore, Frank J.: The Dynamic Motion of a Missile Descending Through the Atmosphere. Jour. Aero. Sci., vol. 22, no. 9, Sept. 1955, pp. 628-632, 638.

3. Tobak, Murray, and Allen, H. Julian: Dynamic Stability of Vehicles Traversing Ascending or Descending Paths Through the Atmosphere. NACA TN 4275, 1958.

4. Sommer, Simon C., and Tobak, Murray: Study of the Oscillatory Motion of Manned Vehicles Entering the Earth's Atmosphere. NASA MEMO 3-2-59A, 1959.

5. Gates, C. R.: A Description of a Mars Spacecraft With a Landing Capsule. American Rocket Society paper no. 61-180-1874, June 1961.

6. Peterson, Victor L.: Motions of a Short 10° Blunted Cone Entering a Martian Atmosphere at Arbitrary Angles of Attack and Arbitrary Pitching Rates. NASA TN D-1326, 1962.

7. Ince, E. L.: Ordinary Differential Equations. Dover Publications, 1927.

8. Roy, Maurice: Means and Examples of Aeronautical Research in France at ONERA (The Twenty-Second Wright Brothers Lecture). Jour. Aero/Space Sci., vol. 26, no. 4, April 1959, pp. 193-206.

9. Boutroux, P.: Recherches sur Les Transcendantes de M. Painlevé et L'Étude Asymptotique des Équations Différentielles du Second Ordre. École Normale Supérieure, Annales scientifiques, Ser. 3, vol. 30, 1913, pp. 256-375, and Ser. 3, vol. 31, 1914, pp. 100-159.

10. Remmler, Karl L.: Tumbling Bodies Entering the Atmosphere. ARS Jour., vol. 32, no. 1, Jan. 1962, pp. 92-95.

11. Jeffreys, Harold, and Jeffreys, Bertha Swirles: Methods of Mathematical Physics. Second Ed., Cambridge Univ. Press, 1950.

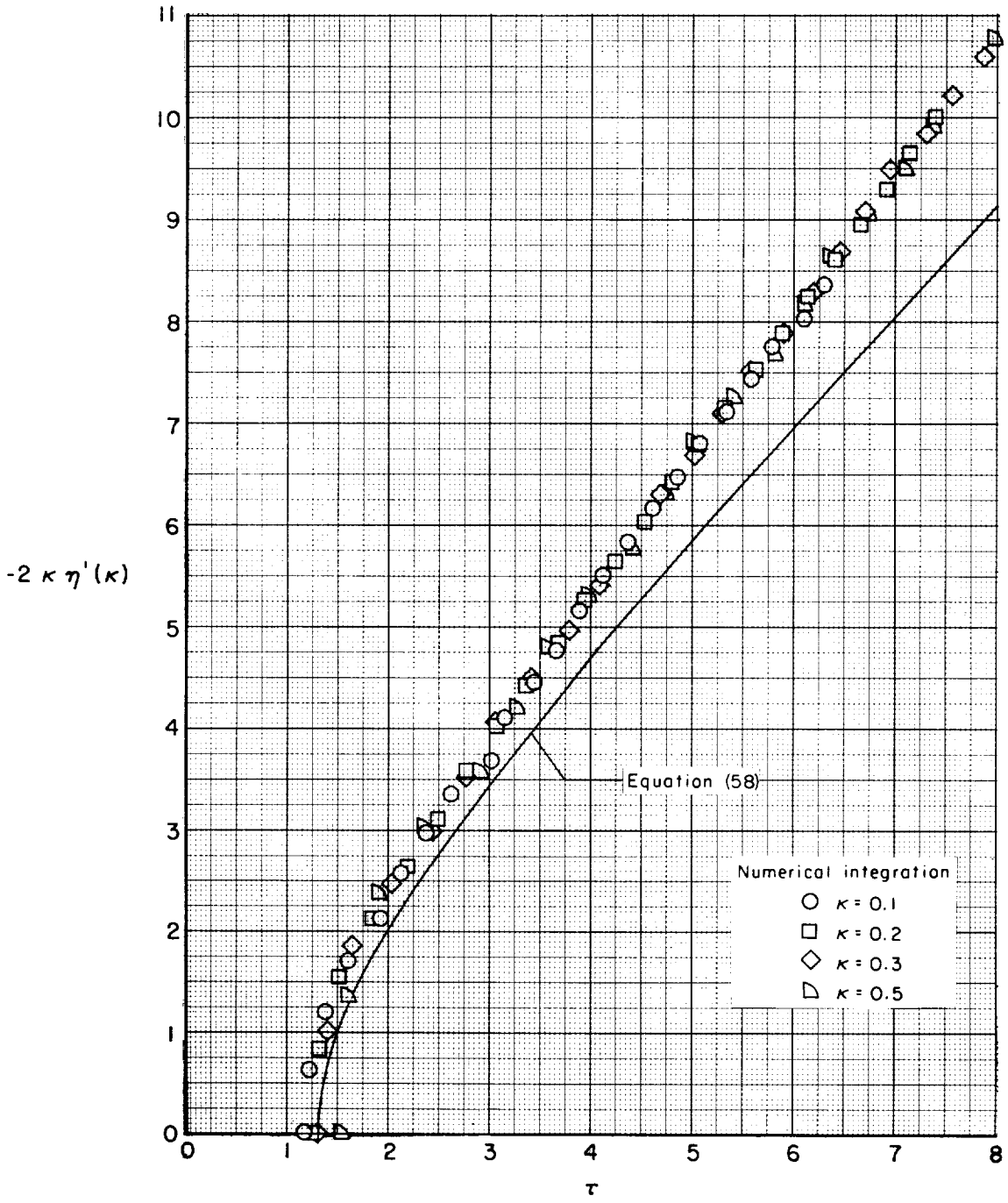

Figure 1.- Variation of $-2\kappa\eta'(\kappa)$ with τ for several values of κ.

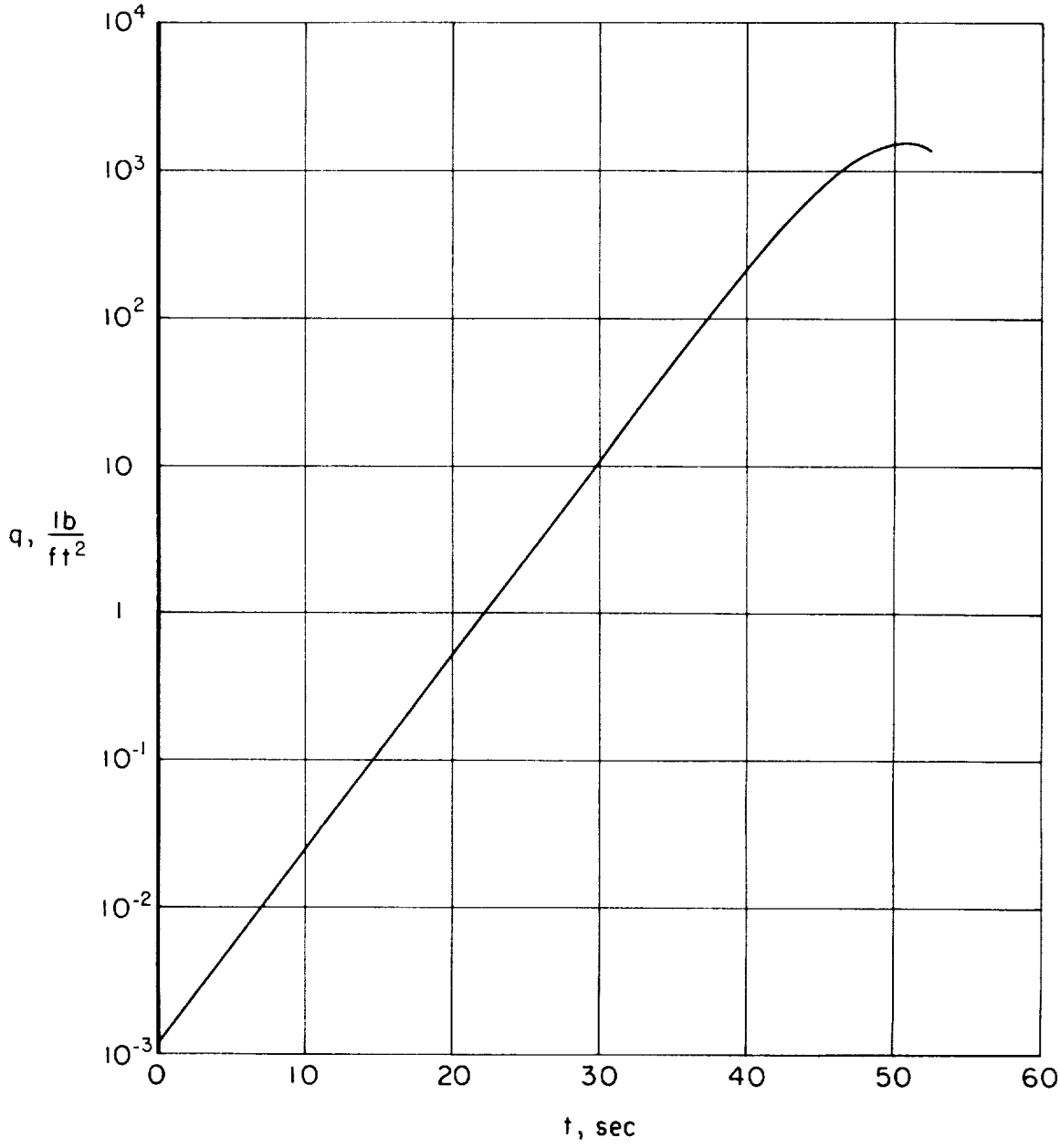

Figure 2.- Initial portion of the dynamic pressure history for a vehicle entering the Martian atmosphere.

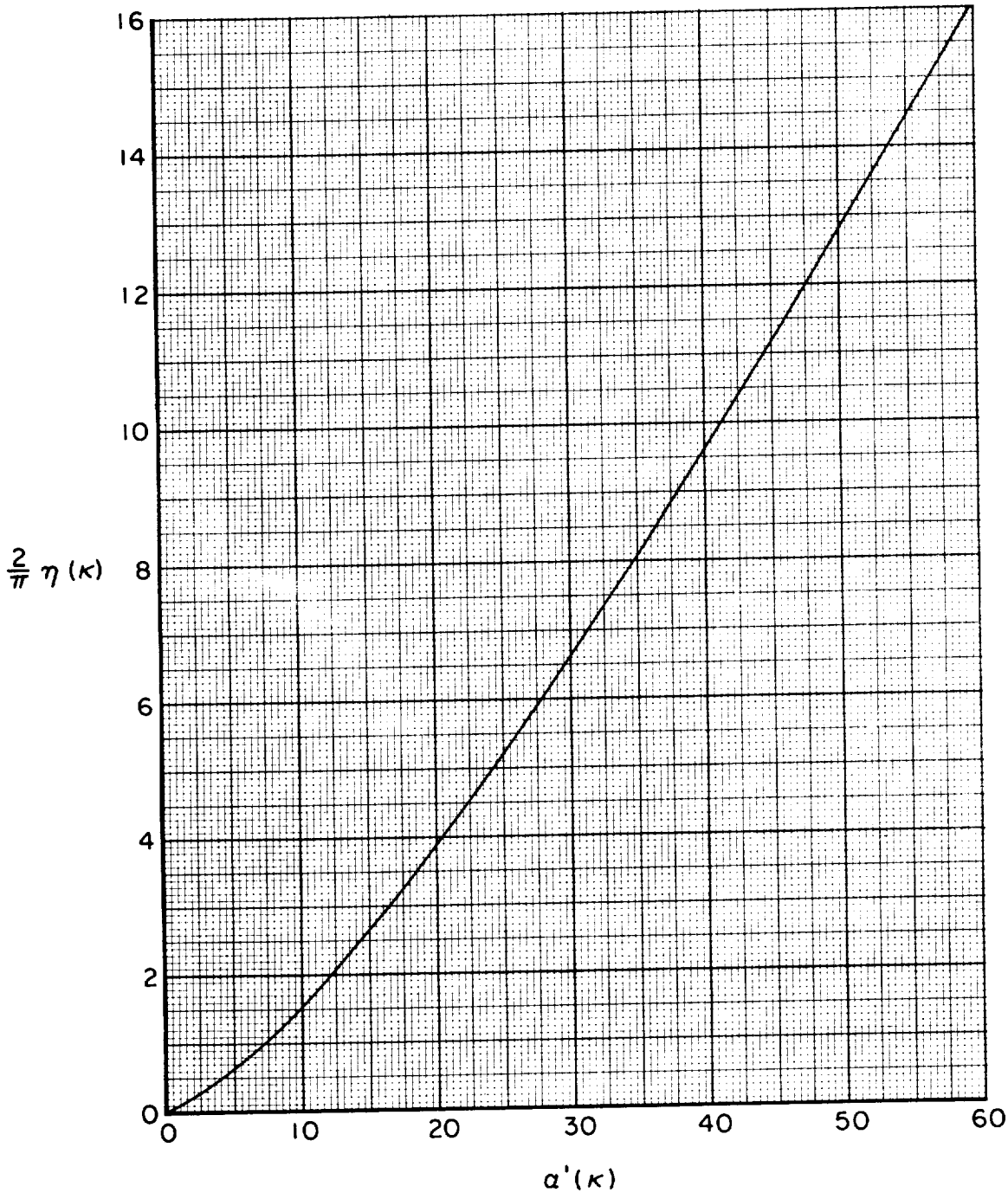

Figure 3.- Variation of $\eta(\kappa)$ with $\alpha'(\kappa)$ for $\kappa = 0.222$.

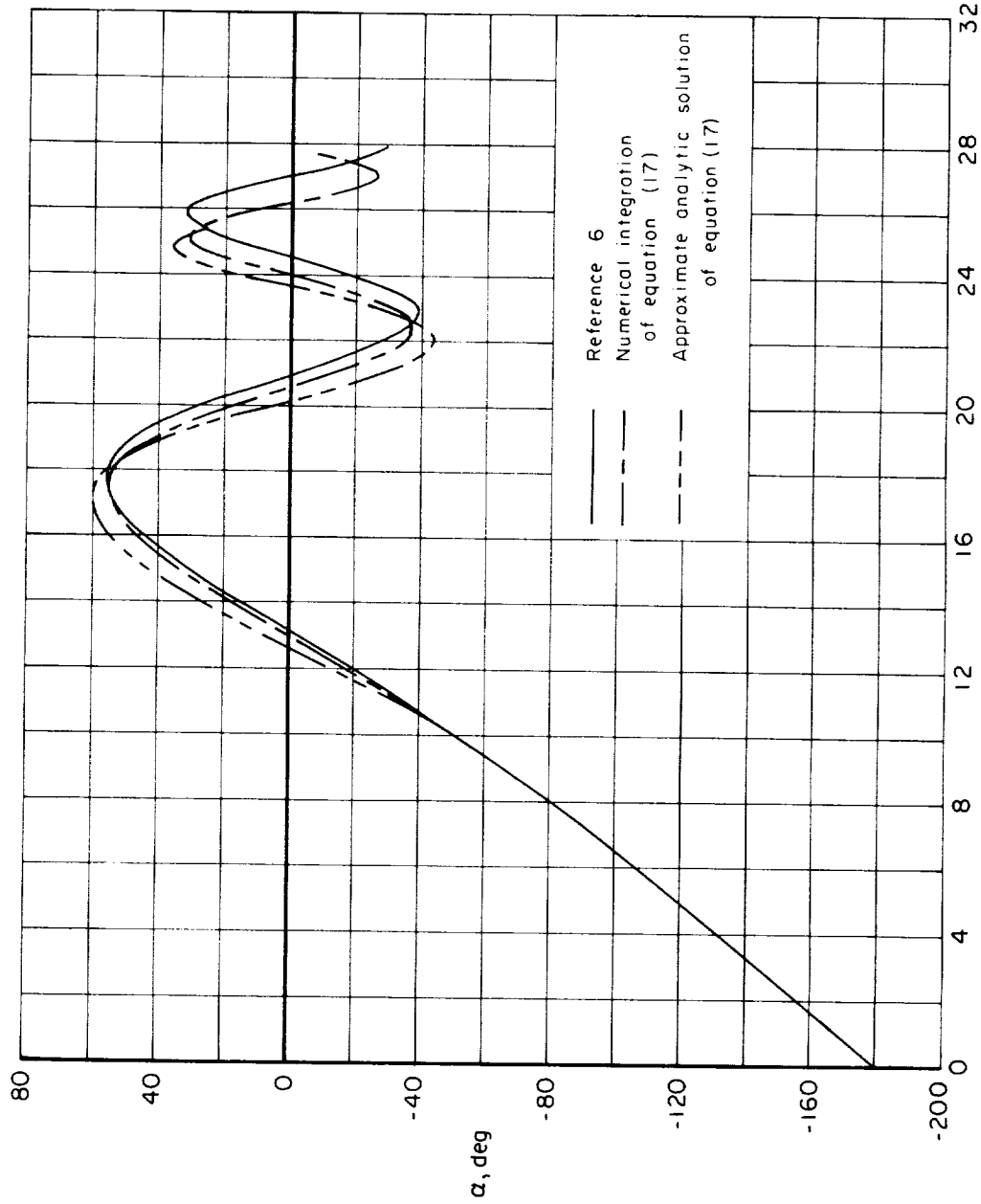

Figure 4.- Comparison of angle-of-attack histories for a vehicle entering the Martian atmosphere; $\alpha_i = -\pi$, $\dot{\alpha}_i = 12^{\circ}/\text{sec}$.

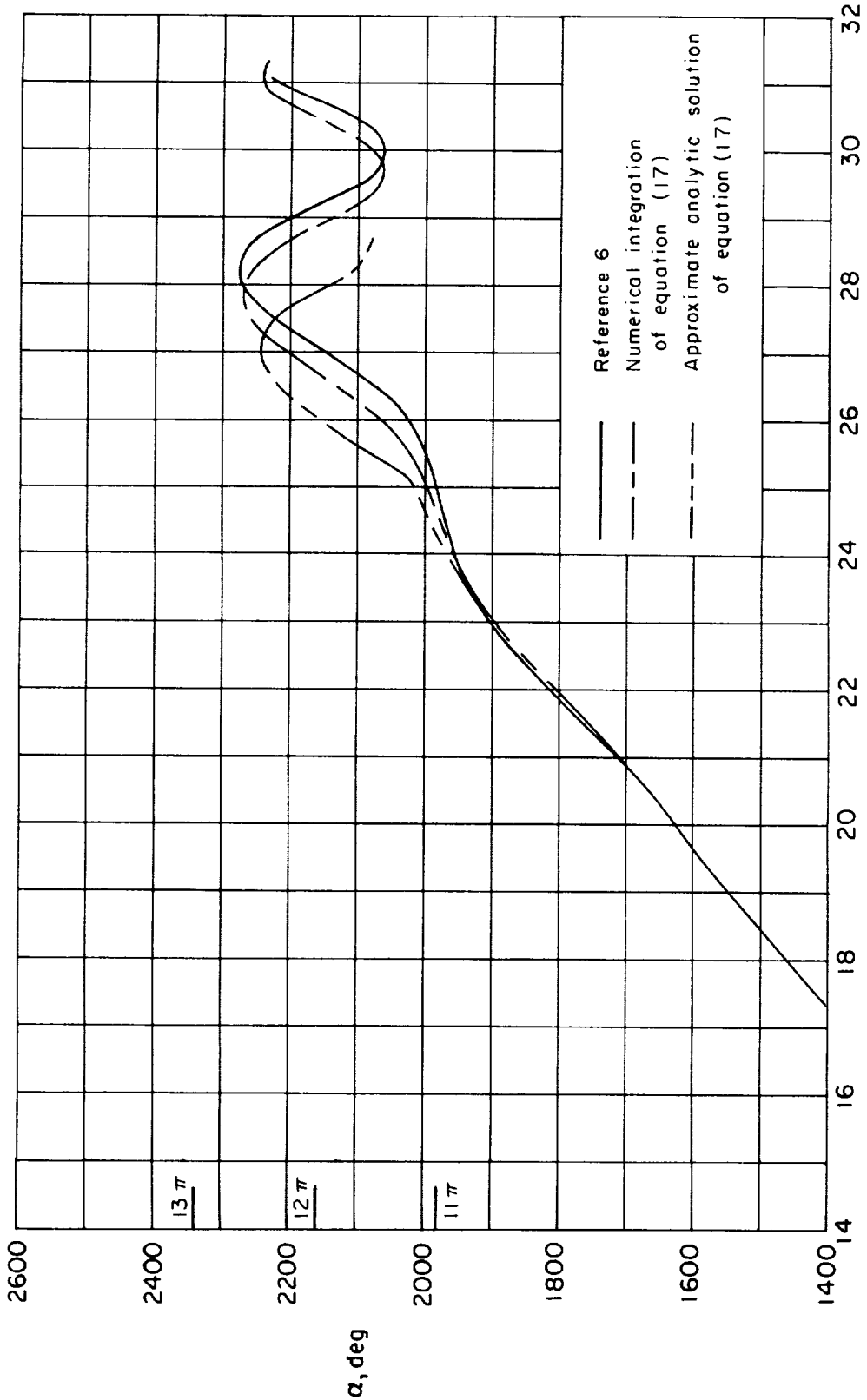

Figure 5.- Comparison of angle-of-attack histories for a vehicle entering the Martian atmosphere; $\alpha_i = 0$, $\dot{\alpha}_i = 86°/sec$.

NASA-Langley, 1962 A-661